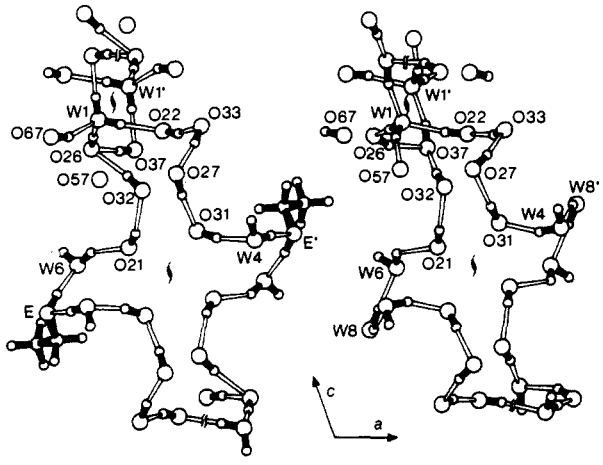


Figure 4. Comparison of hydrogen-bonding structure around $a = {}^1/_2$ for (left) β-CD·EtOD·8$D_2O$ and (right) β-CD·11$D_2O$.

bonding networks in which the homodromic orientation is the dominating theme due to the cooperative effect that strengthens O—H···O bonds in homodromic chains by ~25% relative to the isolated hydrogen bond.[17,18]

The similarity of the hydrogen-bonding patterns in β-CD·11$D_2O$ and β-CD·EtOD·8$D_2O$ and the dominance of the homodromic arrangement suggest that the latter has a decisive influence on the crystallisation of these complexes. The fact that the O—D···O directions can be reversed although the positions of the O atoms are nearly equivalent indicates that the reversal can occur easily. It may be promoted by disorder in the β-CD cavity, which is initiated above a transition temperature (203 K in β-CD·11$D_2O$[9]) and propagates by the formation of flip-flop disordered hydrogen bonds.

**Acknowledgment.** These studies were supported by the Bundesminister für Forschung und Technologie, FKZ 03 SA1 FUB 6, and by Fonds der Chemischen Industrie.

**Supplementary Material Available:** Listing of atomic coordinates and anisotropic temperature factors, individual bond distances, bond angles, and torsion angles for β-CD, ethanol, and water molecules, Cremer and Pople puckering parameters, and coordination geometry for the water molecules (16 pages); tables of structure factor amplitudes (27 pages). Ordering information is given on any current masthead page.

(17) Lesyng, B.; Saenger, W. *Biochem. Biophys. Acta* **1981**, *678*, 408-413.
(18) Koehler, J. E. H.; Saenger, W.; Lesyng, B. *J. Comput. Chem.* **1987**, *8*, 1090-1098.

# Structure and Dynamic Behavior of Solvated Neopentyllithium Monomers, Dimers, and Tetramers: $^1H$, $^{13}C$, and $^6Li$ NMR

**Gideon Fraenkel,* Albert Chow, and William R. Winchester**

*Contribution from the Department of Chemistry, The Ohio State University, Columbus, Ohio 43210.* *Received December 29, 1989*

**Abstract:** NMR studies of neopentyllithium-$^6Li$, Np$^6$Li, in the presence of a variety of solvents and potential ligands reveal four species of unknown aggregation in methylcyclohexane-$d_{14}$, dimers and tetramers in toluene-$d_8$–diethyl-$d_{10}$ ether, dimers in diethyl-$d_{10}$ ether, and monomers and dimers in THF-$d_8$. The thermodynamic parameters for the latter equilibrium are $\Delta H = -1.4$ kcal and $\Delta S = -11.4$ eu toward the monomer. States of aggregation are inferred from the multiplicity of the $^{13}C$ resonance for carbon bound to lithium-6. In bulk THF Np$^6$Li does not complex with TMEDA or 1,2-di(*N*-piperidino)ethane, within the limits of NMR detection. However in the presence of the triamines pentamethyldiethylenetriamine (PMDTA) or 1,4,7-trimethyl-1,4,7-triazacyclononane (TMTAN) in diethyl-$d_{10}$ ether or THF-$d_8$, Np$^6$Li forms tridentate complexed monomers between which interaggregate carbon–lithium bond exchange and lithium–nitrogen coordination exchange are much slower than among the etherate or THF complexes. Carbon-13 NMR of the Np$^6$Li·PMDTA complex in diethyl-$d_{10}$ ether at 150 K shows all but two of the PMDTA carbons to be magnetically nonequivalent, implying that the system exists as one rotamer about the $C_\alpha$–Li bond and that rotation about this bond is slow relative to the NMR time scale at this temperature. In this system we observe $^{13}C$ line-shape changes above 150 K indicative of faster C–Li bond rotation with $\Delta H_r^\ddagger = 7.7$ kcal and $\Delta S_r^\ddagger = -8.8$ eu and then, above 180 K, fast inversion at the $N(CH_3)_2$ nitrogens with $\Delta H_i^\ddagger = 8.7$ kcal and $\Delta S_i^\ddagger = -3$ eu. The latter process appears to be concerted with the exchange of lithiums between Np$^6$Li·PMDTA monomer and Np$^6$Li etherate dimer, as determined from the $^6$Li NMR line shapes. The monomeric complex Np$^6$Li·TMTAN shows two triamine $^{13}CH_2$ carbon resonances, of equal amplitude, which support the proposed conformation of the TMTAN.

The broad outlines of organolithium aggregation are well-known.[1,2] Unsolvated primary $(RLi)_n$ species are hexamers,[3,4] octamers,[4] and nonamers;[4] for the secondary species[5] $n = 4$ and 6 while the more hindered tertiary reagents are largely tetramers.[3b,5b,6] Organolithiums solvated by monoethers (except THF) and tertiary monoamines are largely tetramers.[7] In THF *n*-butyllithium forms equilibrium mixtures of dimers and tetramers[7] with the dimers favored at low temperature.[8] However, the more

(1) Reviewed: (a) Wardell, J. L. In *Comprehensive Organometallic Chemistry*; Wilkinson, G., Stone, F. G. A., Abel, E. W., Eds.; Pergammon Press: Oxford, 1982; Vol. 1, p 43. (b) Wakefield, B. J. *The Chemistry of Organolithium Compounds*; Pergamon Press: Oxford, 1974.
(2) (a) Fraenkel, G.; Hsu, H.-P.; Su, B. M. In *Lithium: Current Applications in Science, Medicine and Technology*; Bach, R. O., Ed.; John Wiley: New York, 1985; p 273. (b) Fraenkel, G. In *Recent Advances in Anionic Polymerization*; Hogen-Esch, T., Smid, J., Eds.; Elsevier: New York, 1987; p 23.
(3) (a) Margerison, D.; Newport, J. P. *Trans. Faraday Soc.* **1963**, *59*, 2058. (b) Brown, T. L. *Acc. Chem. Res.* **1968**, *23*, 1. (c) Beckenbaugh, W.; Fraenkel, G.; Yang, P. P. *J. Am. Chem. Soc.* **1976**, *98*, 6878.
(4) Fraenkel, G.; Henrichs, M.; Hewitt, J. M.; Su, B. M.; Geckle, M. J. *J. Am. Chem. Soc.* **1980**, *102*, 3345-3350. (b) Fraenkel, G.; Fraenkel, A. M.; Geckle, M. J.; Schloss, F. *J. Am. Chem. Soc.* **1979**, *101*, 4745-4747.
(5) (a) Fraenkel, G.; Henrichs, M.; Hewitt, M.; Su, B. M. *J. Am. Chem. Soc.* **1984**, *106*, 255. (b) Thomas, R. D.; Jensen, R. M.; Young, T. C. *Organometallics* **1987**, *6*, 565.
(6) (a) McKeever, L. D.; Waack, R. *Chem. Commun.* **1969**, 751. (b) Thomas, R. D.; Clark, M. T.; Jensen, R. M.; Young, T. C. *Organometallics* **1986**, *5*, 1851. (c) Weiner, M.; Vogel, C.; West, R. *Inorg. Chem.* **1962**, *1*, 654.
(7) (a) Novak, D. P.; Brown, T. L. *J. Am. Chem. Soc.* **1972**, *94*, 3793. (b) McKeever, L. D.; Waack, R.; Doran, M. A.; Baker, E. B. *J. Am. Chem. Soc.* **1969**, *91*, 1057; **1968**, *90*, 3244. (c) West, P.; Waack, R. *J. Am. Chem. Soc.* **1967**, *89*, 4395. (d) Rochonov, A. N.; Shigarin, D. N.; Talaleeva, T. L.; Tsareva, G. V.; Kocheshkov, K. A. *Zh. Fiz. Khim.* **1966**, *40*, 2265.

0002-7863/90/1512-6190$02.50/0 

hindered *sec*-butyllithium is a dimer exclusively, solvated by THF.[9] Dimers are also favored at low temperature for organolithium compounds complexed to TMEDA.[2,9,10] Most recently it has been reported that several organolithium compounds form tridentate monomeric complexes with pentamethyldiethylenetriamine.[9-12] These generalizations come from disparate studies of different RLi species using relatively few potential lithium ligands but never the same actual set.

In this article we report studies of neopentyllithium-$^6Li$, Np$^6$Li, in hydrocarbon solvents and in the presence of a variety of potential ligands. Neopentyllithium is easily prepared in pure state[13] and can be stored, solvent free, indefinitely at room temperature under an inert atmosphere. Lithium-6 ($I$ = 1) has been used since its relaxation rate is slow enough[14] to allow observation of $^{13}$C, $^6$Li scalar couplings, as low as 2 Hz.[4,5,8a,b] Further, from the multiplicity of the $^{13}C_\alpha$ resonance we can infer the nature of the $(RLi)_n$ aggregates. In contrast, the higher (factor of 91) electric quadrupole moment of $^7$Li ($I = {}^3/_2$), versus $^6$Li, is responsible for its fast relaxation rate, which often averages out the $^{13}$C, $^7$Li coupling.[4b] This largely precludes the use of R$^7$Li species in NMR studies of organolithium structure.

All the studies reported here have been initiated at as low a temperature as is consistent with good NMR resolution and to minimize signal-averaging effects due to interaggregate carbon–lithium bond exchange and/or lithium–ligand coordination exchange.[2,8a,b] In sum, the multiplicities of the $^{13}C_\alpha$ resonances at low temperature are expected to reveal structures of aggregates. At higher temperatures NMR line-shape analysis of the signal averaging[16] mentioned above leads in favorable circumstances to kinetic and mechanistic information on the accompanying exchange processes.[17]

## Results and Discussion

For convenience the structures of potential ligands used in this work are listed in one place as **1** to **6** together with their common

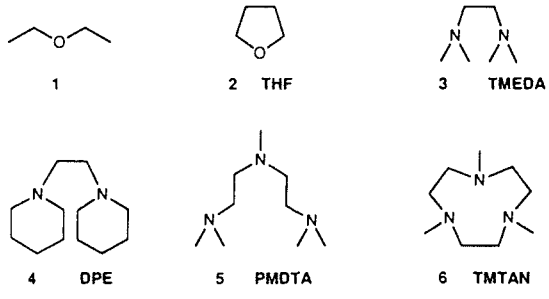


abbreviations, where appropriate. Throughout this paper neopentyllithium-$^6Li$ will be referred to as Np$^6$Li.

Neopentyllithium, Np$^6$Li, was prepared by cleaving dineopentylmercury with $^6$Li (96% $^6$Li, 4% $^7$Li) chips in pentane at room temperature. The white powdered neopentyllithium which remained after removing the solvent has been stable for over a year in a stoppered container in the drybox under argon. A solution of Np$^6$Li in methylcyclohexane-$d_{14}$ stored at room temperature has also been stable ever since it was prepared, over a year. Solutions of Np$^6$Li in ethers (neat diethyl ether or THF) or with tertiary amines are stable for at least 2 weeks at 200 K and sometimes longer, long enough to carry out useful NMR studies reported here.

Neopentyllithium is soluble in methylcyclohexane-$d_{14}$ down to 240 K, below which temperature it precipitates out as an amorphous powder. Carbon-13 resonance of $CH_2Li$ in these solutions did not show $^{13}$C, $^6$Li coupling so no conclusions can be drawn regarding the states of aggregation of neopentyllithium. However, three kinds of NMR data (proton, $^{13}$C, and $^6$Li) reveal the presence of at least four species which most likely differ in their states of aggregation (see Figure 1). This is reminiscent of reports in the literature, based on $^{13}$C NMR data, that several other unsolvated primary alkyllithiums exist as equilibrium mixtures of, for example, as many as 11 species, as assumed by ethyllithium in cyclopentane.[2b] Propyllithium in cyclopentane was

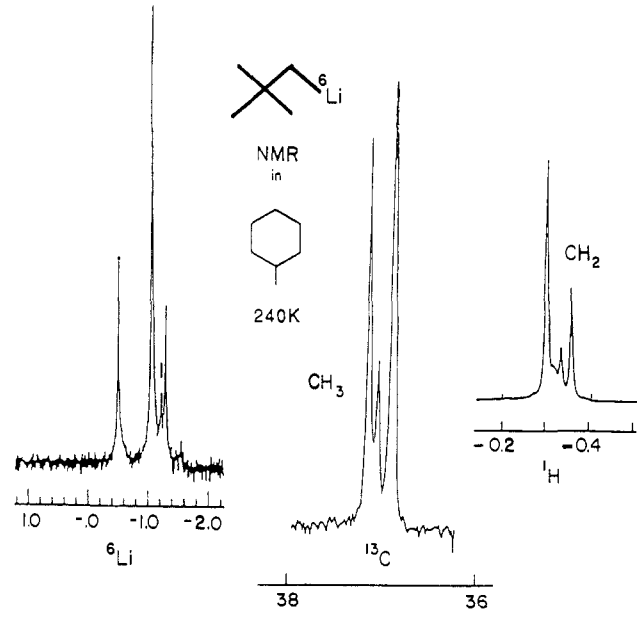


**Figure 1.** $^1$H (300 MHz), $^{13}$C (75 MHz), and $^6$Li (44 MHz) NMR of Np$^6$Li (0.6 M) in methylcyclohexane-$d_{14}$, 240 K.

**Table I.** $^{13}$C NMR of Neopentyllithium-$^6Li$ in Different Media

| concn RLi (ligand) | medium ($T$, K) | species | shifts, δ $CH_3$ | shifts, δ $C_q$ | shifts, δ $CH_2$ | $J$, Hz $^{13}C_\alpha{}^6Li$ |
|---|---|---|---|---|---|---|
| 0.15 | toluene-$d_8$ + | tet | 37.0 | 34.4 | 32.4 | |
| (0.13) | $Et_2O$-$d_{10}$ (150) | dim | 37.9 | 35.0 | 34.8 | 7.6 |
| 0.38 | $Et_2O$-$d_{10}$ (150) | dim | 37.46 | 34.62 | 34.4 | 8.9 |
| 0.02 | THF-$d_8$ (150) | mon | 39.3 | 35.9 | 35.8 | 14.5 |
| | | dim | 38.2 | 35.2 | 33.9 | 7.2 |
| 0.27 | THF-$d_8$ + | mon | 39.2 | 35.7 | 36.6 | 15.0 |
| (0.55) | TMEDA (150) | dim | 37.9 | 35.0 | 33.2 | |
| 0.40 | THF-$d_4$ + | mon | 38.7 | 35.4 | 35.6 | |
| (0.60) | DPE[a] (150) | dim | 37.8 | 34.7 | 33.0 | |
| 0.26 | THF-$d_8$ + | mon | 39.1 | 38.9 | 36.9 | 14.7 |
| (0.32) | PMDTA (170) | | | | | |
| 0.30 | $Et_2O$-$d_{10}$ + | mon | 38.7 | 35.7 | 36.9 | 14.7 |
| (0.17) | PMDTA (170) | dim | 37.6 | 34.8 | 34.4 | |
| 0.53 | THF-$d_8$ + | mon | 39.7 | 36.1 | 35.3 | 15.5 |
| (1.06) | TMTAN | | | | | |
| 0.39 | $Et_2O$-$d_{10}$ + | mon | 37.5 | 34.7 | 35.1 | |
| (0.52) | TMTAN | | | | | |

[a] DPE = dipiperidinoethane.

(8) (a) Heinzer, J.; Oth, J. F. M.; Seebach, D. *Helv. Chim. Acta* **1985**, *68*, 1848. (b) Seebach, D.; Haessig, R.; Gabriel, J. *Helv. Chim. Acta* **1983**, *66*, 308. (c) McGarrity, J. F.; Prodolliet, J.; Smith, T. *Org. Magn. Reson.* **1981**, *17*, 59. (d) McGarrity, J. F.; Ogle, C. A. *J. Am. Chem. Soc.* **1985**, *107*, 1805. (e) McGarrity, J. F.; Ogle, C. A.; Brich, Z.; Loosli, H. R. *Ibid.* **1985**, *107*, 1810.

(9) Bauer, W.; Winchester, W. R.; Schleyer, P. v. R. *Organometallics* **1987**, *6*, 2371.

(10) Crystal structures reviewed: Setzer, W. N.; Schleyer, P. v. R. *Adv. Organomet. Chem.* **1985**, *24*, 353.

(11) (a) Lappert, M. F.; Engelhardt, L. M.; Raston, C. L.; White, A. H. *J. Chem. Soc., Chem. Commun.* **1982**, 1323. (b) Buttrus, N. H.; Eaborn, C.; Hitchcock, P. B.; Smith, J. D.; Stamper, J. G.; Sullivan, A. C. *J. Chem. Soc., Chem. Commun.* **1986**, 969. (c) Schumann, U.; Kopf, J.; Weiss, E. *Angew. Chem.* **1985**, *97*, 222.

(12) Fraenkel, G.; Winchester, W. R. *J. Am. Chem. Soc.* **1988**, *110*, 8720.

(13) Schrock, P. R.; Fellmann, J. D. *J. Am. Chem. Soc.* **1978**, *100*, 3359.

(14) Wherli, F. W. *J. Magn. Reson.* **1978**, *30*, 193.

(15) Pople, J. A.; Schneider, W. G.; Bernstein, H. J. *High Resolution Nuclear Magnetic Resonance*; McGraw-Hill: New York, 1959; p 480.

(16) Kaplan, J. I.; Fraenkel, G. *NMR of Chemically Exchanging Systems*; Academic Press: New York, 1980; Chapter 6.

(17) Fraenkel, G. In *Investigations of Rates and Mechanisms of Reactions*; Bernasconi, C. F., Ed.; John Wiley: New York, 1986; Part II, pp 571-577.

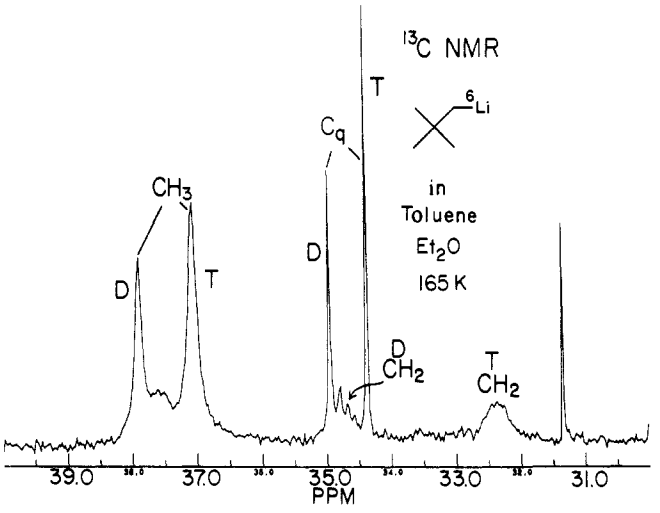


**Figure 2.** $^{13}$C NMR of Np$^{6}$Li (0.15 M) with diethyl-$d_{10}$ ether (0.13 M) in toluene-$d_8$, 165 K; D dimer, T tetramer.

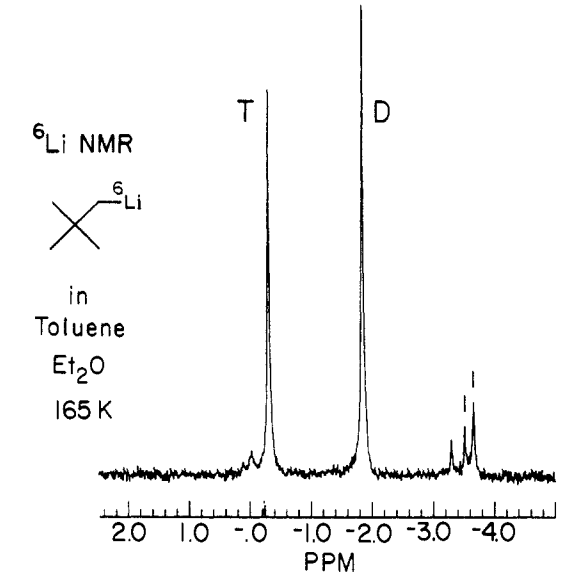


**Figure 3.** Sample described in Figure 2 caption: $^{6}$Li NMR, 44 MHz, 165 K; weak resonances at −3 to −4 ppm due to impurities.

shown to consist of hexamers, octamers, and three kinds of nonamers.[4] In contrast, butyllithium which does not exhibit $^{13}$C, $^{6}$Li coupling forms hexamers in noncoordinating media as well as in the gas phase.[3,6a] Owing to steric destabilization of the hexamers, unsolvated secondary $(RLi)_n$ species form hexamers and tetramers in equilibrium,[5] and finally the tertiary alkyllithiums (unsolvated) give exclusively tetramers.[6]

By way of introduction, Table I outlines the results for coordinated neopentyllithium in several media listed in order of decreasing strength of complexation. In ether–toluene there are dimers and tetramers, but in ether alone, only dimers. In THF-$d_8$ or THF-$d_8$ with TMEDA, we observe dimers and monomers, the ratio (D)/(M) decreasing as the sample is cooled. This latter behavior parallels the solvation behavior of *tert*-butyllithium[9] in contrast to *n*-butyllithium which forms the next larger aggregates with THF, dimers, and tetramers[8] but tetramers only in diethyl ether.[7] Then it would appear that similar steric interactions must be responsible for the small ether solvates formed by Np$^{6}$Li and *tert*-butyllithium.

Finally in the presence of two triamines, neopentyllithium forms monomers exclusively; see Table I. As explained above, these assignments of structure come first from the multiplicity of the $^{13}$C resonance for carbon bonded to $^{6}$Li.[2,4,8a,b] In addition one can see among these data that the $^{13}C_\alpha$, $^{6}$Li coupling constant is approximately inversely proportional to the number of nearest-neighbor lithiums to $^{13}C_\alpha$, N, in an $(RLi)_n$ aggregate, as noted previously,[9] and thus to the degree of aggregation, as

$$J(^{13}C,^{6}Li) = (16 \pm 2)/N$$

is also the $^{13}C_\alpha$ shift. Comparing all these parameters together among the data in Table I leads to the aggregation assignments. Thus one can assign association numbers even when $^{13}C_\alpha$, $^{6}$Li coupling is not observed.

In toluene-$d_8$ with one equiv of diethyl-$d_{10}$ ether at 165 K, Np$^{6}$Li (0.15 M) exhibits dimer and tetramer resonances as explained above (see Table I and Figure 2), with the dimer fraction decreasing only slightly on raising the temperature. Also by 240 K the two sets of resonances have averaged to a single line due to fast interaggregate C–Li bond exchange. The same effects are seen in $^{6}$Li NMR, with two sharp lines at 160 K separated by 0.55 ppm (Figure 3). On warming the sample, these lines also broaden, coalesce, and average by 210 K. Line-shape analysis of the $^{6}$Li data obtained at 190 K yields a $\tau^{-1}$ for dimer of 10.3 s$^{-1}$ under these conditions.[16]

Since almost all diethyl ether is complexed to lithium in these Np$^{6}$Li toluene–diethyl ether solutions, it is not surprising that the NpLi dimer–tetramer ratio, obtained from peak integrations, changes so little throughout the temperature range investigated. Changing the solvent to pure diethyl-$d_{10}$ ether turns all the neopentyllithium into dimers as evidenced by the single quintet

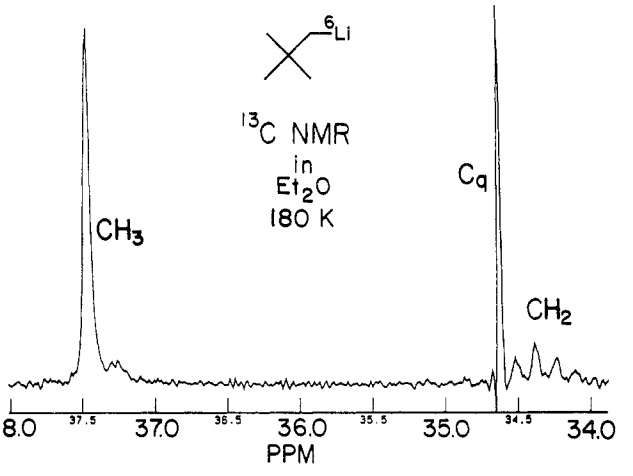


**Figure 4.** $^{13}$C NMR of Np$^{6}$Li (0.38 M) in diethyl-$d_{10}$ ether, 180 K, showing exclusively dimer.

multiplet for $^{13}CH_2$ (Figure 4). These samples show averaging of the $^{13}$C, $^{6}$Li coupling by 190 K. However, the $^{13}C_\alpha$ shift stays constant up to 297 K, implying the predominant species is still dimer up to this temperature.

Neopentyllithium in THF-$d_8$ or THF-$d_4$ gave rise at 150 K to two $^{13}$C NMR spectra (Figure 5). These results are also mirrored in the $^{6}$Li NMR which has two sharp peaks separated by 0.61 ppm at 150 K, which average to a single line by 200 K. As seen from the $^{13}$C, $^{6}$Li coupling constants and $C_\alpha$ resonance multiplicities, one of the species is monomer, M, and the other is dimer, (Table I). The ratio (M)/(D) decreases with increasing temperatue as has been reported for related systems elsewhere. It is generally found that dissociation of organolithium species in coordinating solvents is exothermic because of the extra solvation of lithium required by the less aggregated species.[8,18]

Use of peak area ratios in the $^{13}$C NMR spectra of these neopentyllithium–THF-$d_8$ samples, together with the quantities of NpLi and THF-$d_8$ used, provided concentrations of monomer and dimer at different temperatures. The plot of log (D) versus log (M) for this system at 165 K has a slope of 1.8 ± 0.1 with correlation coefficient of 0.999 58, clearly demonstrating equilibrium between dimer and monomer (eq 1), wherein the number

$$2THF + Np_2Li_2(THF)_4 = 2NpLi(THF)_3 \quad (1)$$

(18) See ref 2b, pp 32–45.
(19) (a) See ref 8a, p 1853. (b) Eaborn, C.; Hitcock, P. B.; Smith, J. D.; Sullivan, A. C. *J. Chem. Soc., Chem. Commun.* **1983**, 827.

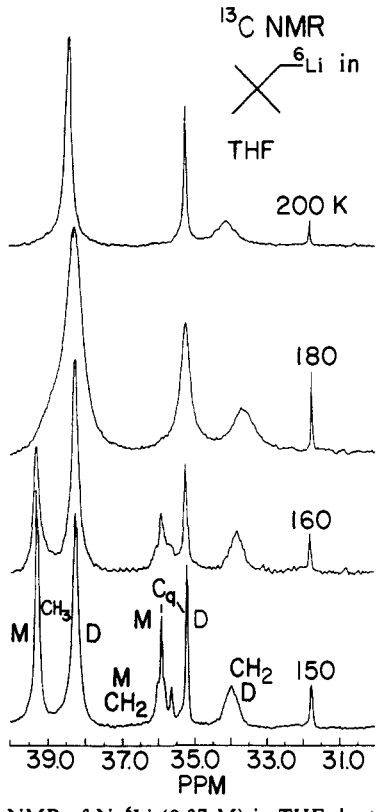


**Figure 5.** $^{13}$C NMR of Np$^{6}$Li (0.37 M) in THF-$d_8$ at different temperatures (K); M monomer, D dimer; peak at $\delta$ 31.8 due to $CH_3$ of neopentane.

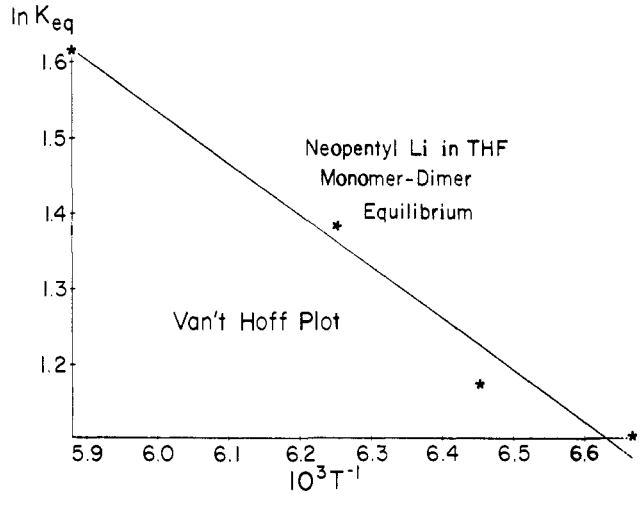


**Figure 6.** Van't Hoff plot for Np$^{6}$Li monomer–dimer equilibrium in THF-$d_8$, dimer direction.

of THF molecules coordinated to different species is assumed from X-ray crystallographic data. Using equilibrium data obtained at four temperatures between 150 and 165 K provides the thermodynamic parameters for equilibrium 1 of $\Delta H = -1.4$ kcal and $\Delta S = -11.4$ eu (see Figure 6). The small, almost neutral enthalpy change resembles that of −2.06 kcal reported by Seebach et al. for dissociation of butyllithium tetramers to dimers in THF, with $\Delta S = -18.8$ eu,[8a] obtained from $^{13}$C NMR data. These results were confirmed by McGarrity and Ogle, who investigated the same equilibrium with $^{7}$Li NMR.[8b] Freezing of the sample below 150 K and signal averaging above 165 K precluded using a wider temperature range to make these measurements for Np$^{6}$Li in THF-$d_8$. In fact, by 210 K the two $^{13}CH_3$ resonances due to monomer and dimer Np$^{6}$Li average to a sharp line with the $^{13}CH_3$ shift close to that of dimer, $\delta$ 38.4. Although the data do not allow accurate calculation of the rate constants for monomer–dimer interconversion, use of the $^{13}$C NMR line shape provides the estimate that at 165 K the mean lifetime for NpLi monomer is 0.075 s$^{-1}$.

Toluene, neat or in diethyl ether solution, is inert to *n*-butyllithium, but on addition of 10 mol % tetramethylethylenediamine, TMEDA, per mole of RLi, metalation of the toluene takes place within 5 min at room temperature.[20] TMEDA favors formation of dimers of RLi species.[2] It has been proposed that the reactive species in the latter and similar reactions is alkyllithium dimer bidentately complexed to TMEDA.[2] As seen in $^{13}$C and $^{6}$Li NMR at different temperatures, Np$^{6}$Li (0.27 M) with TMEDA (0.55 M), in THF-$d_8$ looks very little different from Np$^{6}$Li in THF-$d_8$ alone. Both solutions contain equilibrium mixtures of monomer and dimer NpLi, and the monomer/dimer ratio increases on lowering the temperature. Yet at common temperatures and NpLi concentrations the latter ratio is always slightly larger for the solution containing TMEDA, compared to THF alone. The $^{13}$C shifts for contained TMEDA at $\delta$ 46.4 ($CH_3$) and 58.4 ($CH_2$) are very close to those of free TMEDA, $\delta$ 46.3 ($CH_3$) and 58.8 ($CH_2$). Hence one can assume that in these solutions TMEDA is largely uncomplexed and NpLi is bound to THF-$d_8$.

The sample of Np$^{6}$Li (0.6 M) in THF-$d_8$ with 1,2-dipiperidinoethane[21] (**4**, 0.6 M; see Table I) also contains an equilibrium mixture of monomer and dimer in similar ratio to the solution of Np$^{6}$Li in THF-$d_8$ alone. The $^{13}$C shifts of contained **4** (piperidino counting from N 55.11, 26, 24.38, $CH_2$ acyclic 56.83) are very similar to those of the free diamine (listed in the same order, 55.6, 26.5, 24, and 58.5), all shifts in $\delta$ units. Hence when bulk THF and **4** both compete for lithium, most of the NpLi is complexed to THF.

A solution of Np$^{6}$Li 0.15 M in THF-$d_8$ with pentamethyldiethylenetriamine,[9] (PMDTA, 0.22 M) contains only monomer, within the limits of NMR detection as evidenced by the triplet $^{13}$C resonance for $CH_2$ with $^{13}$C, $^{6}$Li coupling of 14.7 Hz (see Figure 7a). Furthermore, the fact that this splitting only begins to average by 200 K implies the rate of interaggregate carbon–lithium bond exchange is slow relative to this time scale up to this temperature. In the spectrum of this sample the resonances from $\delta$ 49 to 59 come from free and complexed ligand. A DEPT experiment distinguished between $NCH_2$ and $NCH_3$, while comparison with the $^{13}$C NMR of PMDTA in THF at 150 K identified resonances due to free amine. These are $CH_2$, $\delta$ 58.32 and 57.46; $N(CH_3)_2$, $\delta$ 46.20; $NCH_3$, $\delta$ 43.13, all labeled F on Figure 7a. Integration of the remaining ligand peaks shows that they come from a single molecular species in which all carbons are magnetically nonequivalent. These are, in $\delta$ units, 57.19, 56.60, 54.38 and 51.30 for $CH_2$; 47.36, 49.78, 44.60, and 43.13 for $N(CH_3)_2$; and 44.97 for $CH_3N$, labeled C on Figure 7a. Notice that one of the $N(CH_3)_2$ shifts for the complex is coincident with the center $NCH_3$ shift of free amine. From the integration of the spectrum it appears that the ratio of complexed to free amine is 1.5 ± 0.1.

NOE experiments $^{6}$Li{$^{1}$H} with the Np$^{6}$Li–PMDTA–THF sample show enhancements on irradiating $NCH_3$, $CH_2Li$, and $CH_3C$ protons of, respectively, 29.4, 12.3, and 8%.

Taken together, the data for Np$^{6}$Li with PMDTA in THF require the organolithium to be monomeric and in the form on one unsymmetrical conformer about the carbon–lithium bond (see Figure 8). Rotation of coordinated PMDTA with respect to the neopentyl group must the slow relative to the $^{13}$C NMR time scale, the latter being the shifts among nonequivalent pairs of methyls and methylenes.

Above 150 K, with increasing temperature there is line broadening and signal averaging of the $^{13}$C resonances of complexed and free PMDTA due to progressively faster exchange of ligand between its free and complexed states so that by 210 K the PMDTA part of the spectrum has just four $^{13}$C peaks (see Figure 7b). These averaged shifts reflect the same ratio of com-

(20) Langer, A. W. *Trans. N. Y. Acad. Sci., Ser. II* **1965**, *27*, 741.
(21) Halasa, A. F.; Mochel, V. D.; Fraenkel, G. In *Anionic Polymerization: Kinetics, Mechanisms and Synthesis*; McGrath, G. E., Ed.; ACS Symposium Series No. 166; American Chemical Society: Washington, D.C., 1981; p 367.
(22) Kaplan, J. I.; Fraenkel, G. *J. Am. Chem. Soc.* **1972**, *94*, 2907.

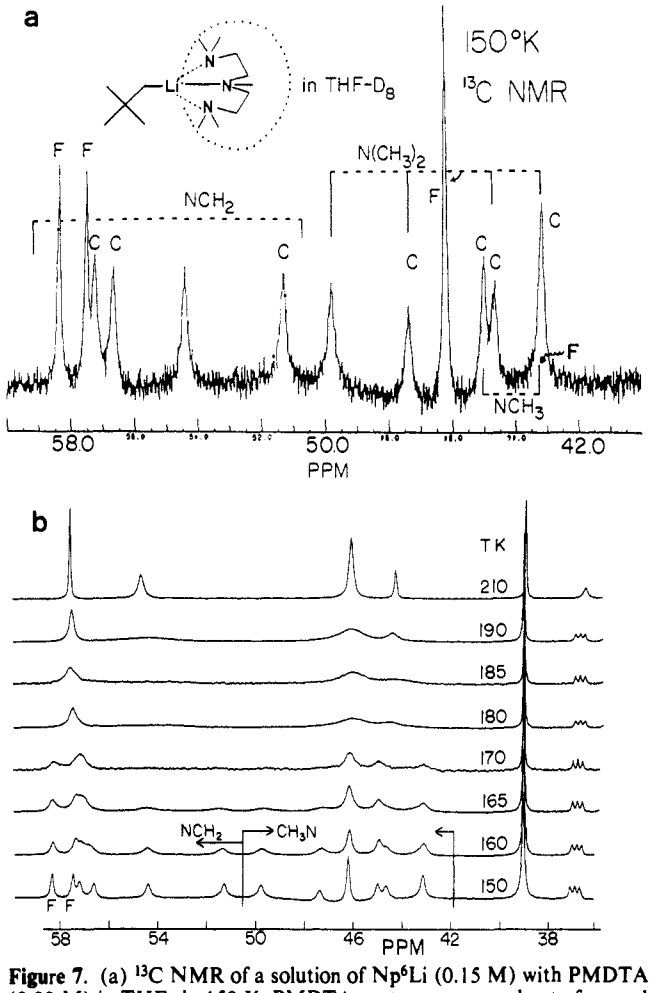


**Figure 7.** (a) $^{13}$C NMR of a solution of Np$^6$Li (0.15 M) with PMDTA (0.22 M) in THF-$d_8$, 150 K, PMDTA part; resonances due to free and complexed PMDTA labeled F and C, respectively. (b) Same sample as (a), entire $^{13}$C NMR different temperatures.

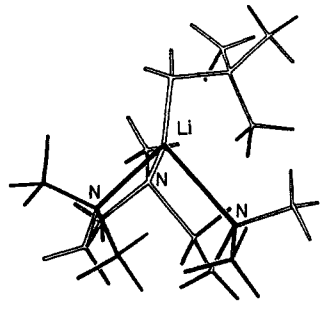


**Figure 8.** Proposed structure of the NpLi·PMDTA complex.

plexed to free PMDTA of 1.5 seen at the lower temperature, previously, by integration. Clarifying which resonances undergo signal averaging also matches resonances for carbons in complexed PMDTA with those in the free ligand. For instance, one can see that $CH_2$'s in complexed PMDTA at $\delta$ 54.34 and 51.03 are equivalent in the free amine at $\delta$ 57.46. From the appearance of these spectra it is not possible to tell whether the averaging of the shifts in free with complexed PMDTA is the result of just one exchange process or whether there are in addition fast rearrangements within the complexed PMDTA which contribute to the changes in the NMR line shape. In fact, we have identified such rearrangements, separately, from $^{13}$C NMR spectra of NpLi with PMDTA in diethyl-$d_{10}$ ether described below.

Carbon-13 NMR at 165 K of Np$^6$Li (0.59 M) with PMDTA (0.34 M) in diethyl-$d_{10}$ ether shows monomers and dimers with characteristic shifts in ratio 1.4/1 (see Table I and Figure 9). The Np$^6$Li dimer resonances have the same shifts as those for Np$^6$Li in diethyl-$d_{10}$ ether alone. Consistent with these results, the $^6$Li

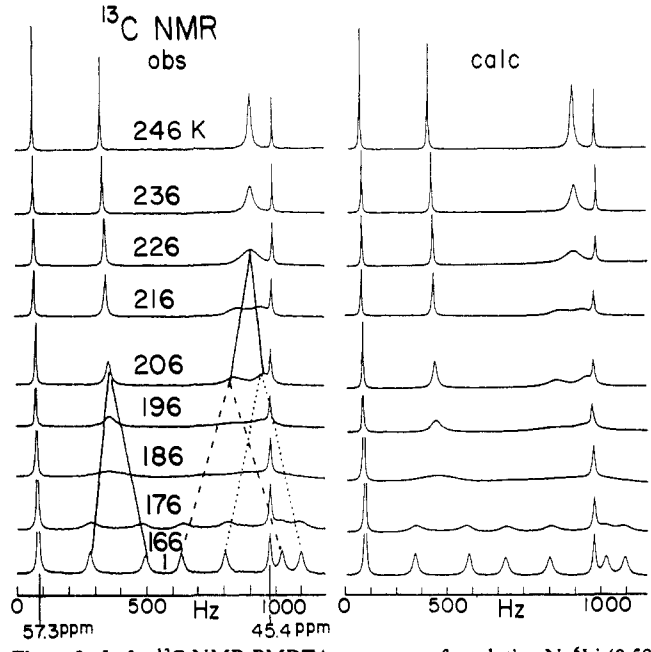


**Figure 9.** Left: $^{13}$C NMR PMDTA resonance of a solution Np$^6$Li (0.59 M) with PMDTA (0.34 M) in diethyl-$d_{10}$ ether at different temperatures, K. Right: Calculated line shape reuslting from rotation about the C–Li axis and nitrogen inversion; see text. Peak assignments are listed in Table II.

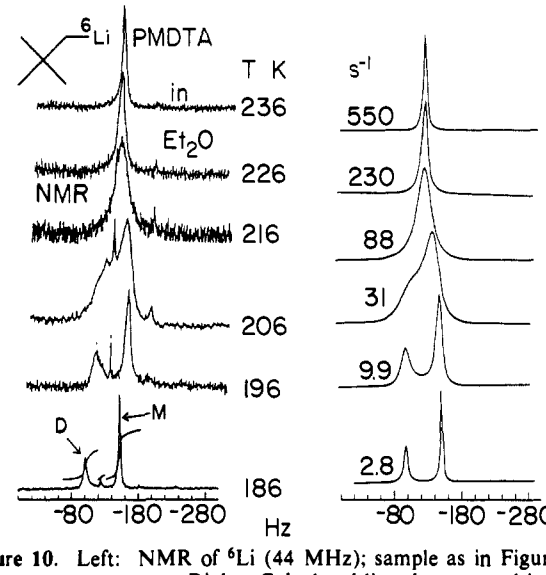


**Figure 10.** Left: NMR of $^6$Li (44 MHz); sample as in Figure 9 at different temperatures. Right: Calculated line shapes, resulting from interaggregate C–Li bond exchange, with first-order rate constants for monomer.

**Table II.** $^{13}$C NMR Shifts ($\delta$) of PMDTA Complexed to Neopentyllithium in $Et_2O$ and THF

| $CH_2$ | | $N(CH_3)_2$ | | $NCH_3$ | |
|---|---|---|---|---|---|
| THF | $Et_2O$ | THF | $Et_2O$ | THF | $Et_2O$ |
| 57.15 | 57.34 (2)[a] | 49.78 | 50.06 | 44.97 | 45.42 |
| 56.11 | | 47.36 | 47.69 | | |
| 54.37 | 54.68 | 44.63 | 44.82 | | |
| 51.29 | 51.86 | 43.13 | 43.85 | | |

[a] Twice the intensity of all other peaks.

NMR of this sample (Figure 10) has two peaks in ratio 1.4/1. Carbon-13 NMR of the contained ligand closely resembles that of the PMDTA complex with Np$^6$Li in THF-$d_8$ (see Table II) with the exception that two of the methylene carbons have the same shift. All the other carbons are well-resolved (Figure 9). No Free PMDTA is detected in this spectrum. Thus by stochiometry the remaining 0.25 M of Np$^6$Li must be complexed

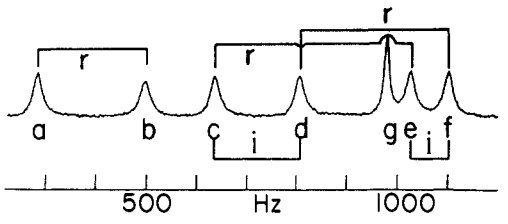


**Figure 11.** Signal averaging scheme due to rotation, r, and nitrogen inversion, i, of PMDTA $^{13}C$ resonances of sample described in Figure 9 caption.

to diethyl-$d_{10}$ ether in the form of dimers, giving a monomer dimer ratio of 1.35, within experimental error of the NMR integrations.

Above 166 K two regimes of signal averaging are seen in the $^{13}C$ NMR of PMDTA complexed to Np$^6$Li in diethyl-$d_{10}$ ether. Two pairs of doublets due to $(CH_3)_2N$ methyls average to broad lines at their respective centers, as do also the methylene pair at $\delta$ 54.68 and 51.86 (see dashed lines in Figure 9). At temperatures above 200 K, the broadened doublet due to the $(CH_3)_2N$ methyls averages to a line at its center. Meanwhile the $NCH_3$ peak remains sharp and unchanged from 166 to 246 K. The symmetrical character of all signal averaging strongly implies that a common monomeric species prevails throughout the entire temperature range investigated.

Turning back to the shapes of the $^{13}C$ spectra in Figure 9, NMR line-shape analysis, described below, shows that the processes responsible for separately averaging the two $N(CH_3)_2$ doublets and the single $CH_2$ doublet over the lower temperature range have the same rates and most likely the same origin. Since the above-mentioned two methylenes are magnetically equivalent in free PMDTA, the averaging of their resonances must be the result of a rearrangement within the complexed monomer specifically rotation about the C–Li bond. Inspection of the proposed monomeric complex reveals that fast rotation about this bond should average the shifts of methyls c and e and, separately, of d with f since rotation necessary passes through a state with a plane of symmetry (see modified Newman projection **7**), in which d, d, e, and f represent the $N(CH_3)_2$ methyls.

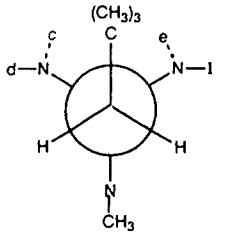


**7**

At higher temperatures, above 200 K, a second slower process averages the broadened doublet due to methyls c + d and e + f, respectively, to a single line at its center. Phenomenologically this must be due to fast inversion at the $N(CH_3)_2$ nitrogens, and that is the temporary label we apply until the origin of this effect is discussed after the section on line-shape analysis which follows.

It is instructive to describe how NMR line-shape analysis[16] has been carried out of the $^{13}C$ resonance of Np$^6$Li complexed PMDTA (described above), taking account of two dynamic processes but without making assumptions about the actual mechanisms involved. The rotational process, r, involves averaging two $CH_2$ peaks a with b (see Figure 11) and $N(CH_3)_2$ resonances c and e and d with f, while nitrogen inversion (slower), i, averages c with d and e with f. Meanwhile, the $NCH_3$ resonance, g, remains unperturbed by these exchange processes but must be included in the calculations since it overlaps with the rest of the spectrum. The system is simulated as a collection of seven uncoupled pseudo-half-spin species. The methylene part is treated separately as a collapsing uncoupled AB doublet. Turning to the methyl resonances, their pseudo-half-spin density matrix elements $\rho_{\alpha,\beta}$ are written as $\rho_c$, $\rho_d$, $\rho_e$, $\rho_f$, and $\rho_g$. The exchange part, $E\rho_x$, of the density matrix equation,

$$\dot{\rho}_x = i[\rho_x, H_x] + E\rho_x + (\rho_x/T) \tag{2}$$

is given as

$$E\rho_x = k_r(\rho_x(ar) - \rho_x) + k_i(\rho_x(ai) - \rho_x) \tag{3}$$

where the $k$'s are pseudo-first-order rate constants, and ai or ar mean respectively, after inversion and after rotation. An element of $E\rho_x$ is written in exactly the same way as (3) since the states $\alpha$, $\beta$ have already been omitted from the $\rho$ symbols. Then, following the averaging connectivities listed above, the $\rho_c(ar)$, $\rho_c(ai)$ elements become

$$\rho_c(ar) = \rho_e \tag{4}$$

$$\rho_c(ai) = \rho_d \tag{5}$$

Examples of density matrix equations are, for $\rho_\omega$,

$$[i(\omega - \omega_d) - (1/T) - k_r - k_i]\rho_d + k_r\rho_f + k_i\rho_c = -iC \tag{6}$$

and for $\rho_e$,

$$[(i(\omega - \omega_e) - (1/T) - k_r - k_i)]\rho_e + k_r\rho_d + k_i\rho_c = -iC \tag{7}$$

where the $\omega_x$'s are shifts in rad s$^{-1}$, $\omega$ is the frequency axis of the spectrum, $1/T$ is the intrinsic line width, and $C$ is the constant on the right-hand side of each equation. Because we are dealing with a first-order system, it is convenient to separate the exchange part **E** of the coefficient matrix **A** (eq 9), of the coupled density matrix equation (eq 8):

$$[\mathbf{A}]\rho_{col} = -iCB_{col} \tag{8}$$

$$\mathbf{A} = \mathbf{\Omega} + \mathbf{R} + \mathbf{E} \tag{9}$$

Since the frequency and relaxation matrix, $\mathbf{\Omega} + \mathbf{R}$, is already diagonal, these latter elements are $i(\omega - \omega_x) - (1/T)$ in the order x = c, d, e, f, and g; the same order applies to $\rho_{col}$, $\rho_c$ to $\rho_g$; $B_{col}$ is just a vector of five ones. The term $\rho_g$ for the $NCH_3$ absorption does not mix with any of the others but must be included since the peak overlaps absorption from the other $\rho$ elements. Finally the exchange matrix is given as (10). Then, given shifts, intrinsic

$$\begin{bmatrix} -k_r-k_i & k_i & k_r & 0 & 0 \\ k_i & -k_r-k_i & 0 & k_i & 0 \\ 0 & 0 & -k_r-k_i & k_i & 0 \\ 0 & k_r & k_i & -k_r-k_i & 0 \\ 0 & 0 & 0 & 0 & 0 \end{bmatrix} = \mathbf{E} \tag{10}$$

line widths, and trial rate constants, the coupled density matrix equations are solved for $\rho_c$ to $\rho_g$, and the absorption is obtained from the summation:

$$\text{Abs}(\omega) = -\text{Im}(\rho_c + \rho_d + \rho_e + \rho_f + \rho_g) \tag{11}$$

Carbon-13 NMR line shapes of coordinated PMDTA (to NpLi) were calculated as a function of $k_r$ and $k_i$ to match the experimental ones. Figure 9 displays the observed spectra together with the line shapes calculated to reproduce them. Eyring plots of the rate constants derived in this way (Figures 12 and 13) give activation parameters $\Delta H_r^\ddagger = 7.7$, $\Delta H_i^\ddagger = 8.7$, both in kcal/mol, and $\Delta S_r^\ddagger = -8.8$, $\Delta S_i^\ddagger = -3$, both in eu.

Whereas the faster dynamic process referred to above is most likely the result of rotation of coordinated lithium about the carbon–lithium bond axis, the origin of the slower inversion process at the $(CH_3)_2N$ nitrogens is still not apparent. Several mechanisms are possible. For example, fast reversible local nitrogen–lithium bond dissociation, alone, would result in fast inversion at nitrogen. Alternatively, the entire complex could undergo inversion at lithium via dissociation of $CH_3N$ off lithium, then recombining on the opposite side (Scheme I). This process would invert the configuration at lithium and all three nitrogens. In fact, neither mechanism obtains; rather nitrogen inversion appears to be coupled to the exchange of lithium (and neopentyls) between monomer and dimer.

Recall that the sample described above of Np$^6$Li with PMDTA in diethyl-$d_{10}$ ether contains monomeric NpLi complexed to PMDTA and dimers of NpLi bound to the ether. No free amine was detected. Because 180 and 250 K the $^{13}C$ resonances for neopentyls in monomer and dimer undergo signal averaging as

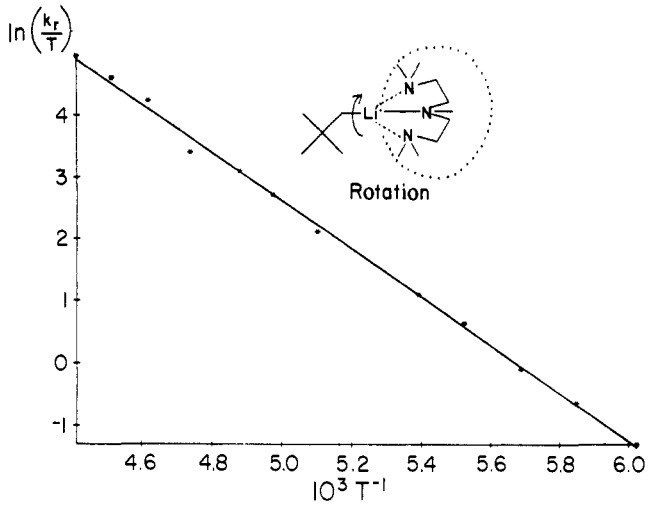


**Figure 12.** Eyring plot for rotation about the lithium–carbon bond in Np$^6$Li·PMDTA in diethyl-$d_{10}$ ether described in caption to Figure 9.

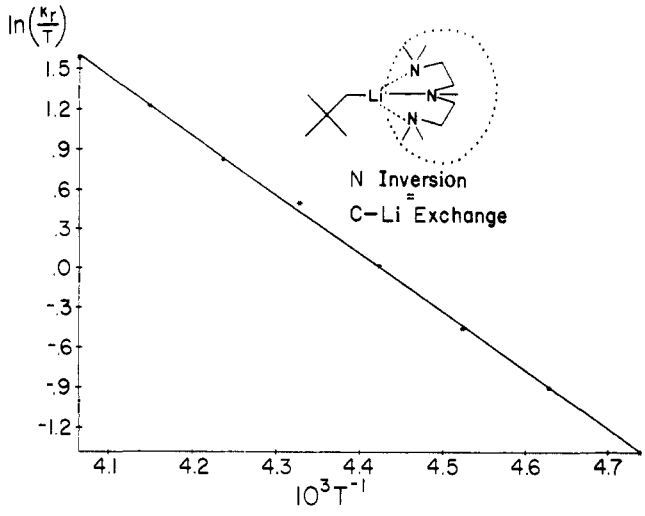


**Figure 13.** Eyring plot for $N(CH_3)_2$ nitrogen inversion in Np$^6$Li·PMDTA; see caption to Figure 9.

**Scheme I**

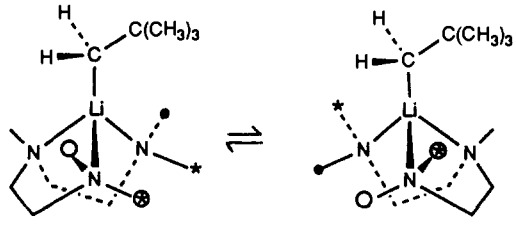

do also the two $^6$Li resonances (see Figure 10). We have simulated[16] the $^6$Li NMR as due to rapid interconversion of monomers and dimers, omitting solvation of both species:

$$D \rightleftarrows 2M \tag{12}$$

As far as $^6$Li NMR is concerned, the equilibrium can be rewritten as

$$^6Li_2 \rightleftarrows 2^6Li \tag{13}$$

We use the spin product representation so states of "Li" and $Li_2$ are written as

$$\phi^D_{Li_2} = \phi_1\phi_2 = ab \tag{14}$$

$$\phi^M_{Li} = \phi = d \tag{15}$$

where the order follows the numbering of the spins, and each lower case letter stands for a state of $^6$Li.

**Table III.** NMR Line-Shape Analysis, $^{13}$C and $^6$Li Neopentyllithium (0.59 M) with PMDTA (0.34 M) in Diethyl-$d_{10}$ Ether

| $T$, K | Li exchange $^6$Li NMR $1/\tau_M$, s$^{-1}$ | N inversion $^{13}$C NMR $1/\tau_i$, s$^{-1}$ |
|---|---|---|
| 186 | 2.8 | 2.8 |
| 196 | 12 | 9.9 |
| 206 | 41 | 31 |
| 216 | 88 | 88 |
| 226 | 230 | 230 |
| 230 | 650 | 550 |

Since the spin of $^6$Li is 1, we require 12 $\Delta m = +1$ elements of the density matrix of "$^6Li_2$" $\rho^D_{ab,a'b'}$ and two for "$^6$Li". The after-exchange (ae) elements from the $E\rho$ term in the density matrix equation, (2), are evaluated for dimer and monomer following the Permutation of Indices[16,21] method as

$$\rho(ae)^D_{ab,ac} = \tfrac{1}{3}\rho^M_{b,c} \tag{16}$$

$$\rho(ae)^M_{d,e} = \sum_f(\rho^D_{df,ef} + \rho^D_{fd,fe}) \tag{17}$$

where the summation is over all (f) states of $^6$Li. Since the $^6$Li NMR of the Np$^6$Li monomer–dimer mixture is a first-order uncoupled system (one peak for each species), the 14 density matrix equations can be contracted to two superelements, one each for monomer and dimer by making the substitution:

$$\rho^D = \sum_{\substack{ab,a'b' \\ \Delta m=+1}} \rho^D_{ab,a'b'} \tag{18}$$

$$\rho^M = \sum_{\substack{d,e \\ \Delta m=+1}} \rho^M_{d,e} \tag{19}$$

the summations being over all pairs of states connected by a $\Delta m = +1$ transition. This procedure gives rise to the density matrix equations in matrix form (eq 20), where the $\Delta\omega_w$'s are shifts in

$$\begin{bmatrix} i\Delta\omega_D - (1/T) & 2/\tau_D \\ -1/\tau_D & \\ & i\Delta\omega_M - (1/T) \\ 1/2\tau_M & -1/\tau_M \end{bmatrix} \begin{bmatrix} \rho^D \\ \\ \rho^M \end{bmatrix} = iC \begin{bmatrix} 1 \\ \\ 1/2 \end{bmatrix} \tag{20}$$

the rotating frame, $\omega - \omega_s$, and $\tau$'s are lifetimes between successive exchanges which are related as in eq (21), the (M)/(D) ratio being

$$\frac{\tau_M}{\tau_D} = \frac{(M)}{(D)} \tag{21}$$

constant over the temperature range utilized. The final absorption comes from summing the superelements, weighted by their respective lithium concentrations:

$$\text{Abs}(\omega) = -\text{Im}((M)\rho^M + (D)\rho^D) \tag{22}$$

Lithium-6 NMR line shapes, calculated according to the procedure just described, are shown in Figure 10 together with the experimental spectra they reproduce. On comparing the rate constants derived for interaggregate lithium exchange with inversion rates at $N(CH_3)_2$ nitrogens (Table III), it is seen that the two processes have very similar rates and most likely come from the same mechanism. Further details as to how this exchange takes place are not evident from the available data; however, some qualitative support comes from $^{13}$C NMR of a sample almost equimolar in Np$^6$Li and PMDTA (both 0.17 M) in diethyl-$d_{10}$ ether. Only Np$^6$Li monomer was observed and dimer could not be detected. This sample shows a well-resolved doublet for the $N(CH_3)_2$ methyls at 220 K, whereas that from NpLi/PMDTA 2:1, also in diethyl-$d_{10}$ ether, has already coalesced by this temperature. Thus qualitatively we see that the rate of inversion at the $N(CH_3)_2$ nitrogens in NpLi·PMDTA is faster in the presence of the Np$^6$Li etherate dimer than in Np$^6$Li·PMDTA alone.

A second system in which Np$^6$Li forms monomers is Np$^6$Li (0.7 M) with 1,4,7-trimethyl-1,4,7-triazacyclononane (6 (TMTAN),

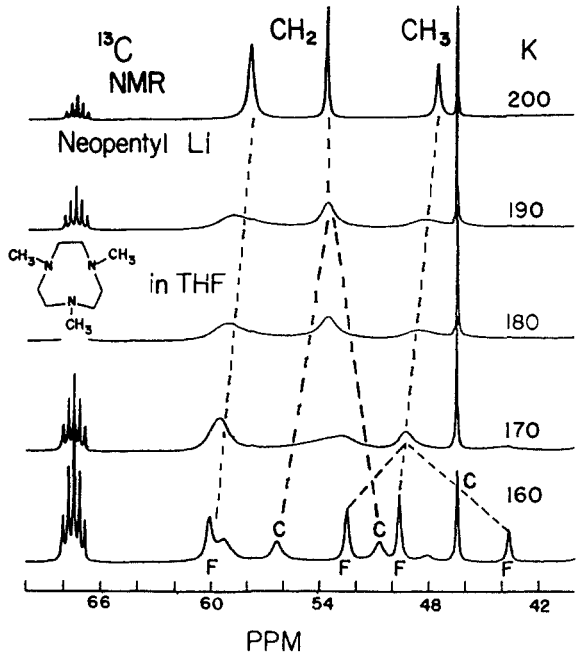


**Figure 14.** $^{13}C$ NMR of Np$^6$Li (0.7 M) with TMTAN (**6**) (1.4 M) in THF-$d_8$, at different temperatures (triamine part only).

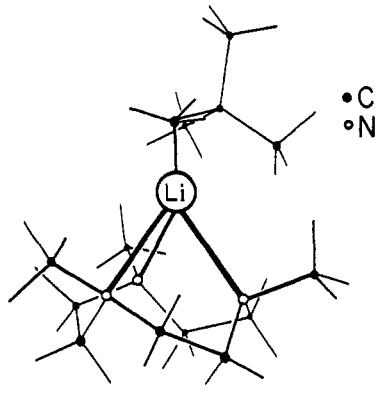


**Figure 15.** Proposed structure of the Np$^6$Li·TMTAN complex using crystallographic bond distances from other complexed monomeric organolithium compounds; see text.

1.4 M) in THF-$d_8$. Carbon-13 NMR of this solution shows only monomer within the limits of NMR detection between 150 and 270 K (Table I), and the splitting of the $^{13}CH_2$ resonance is still seen up to 260 K, implying carbon–lithium bond exchange is slow, at least up to 260 K. Comparing the TMTAN part of the $^{13}C$ NMR at 160 K with that of the TMTAN in THF-$d_8$ alone at the same temperature distinguishes the peaks due to free triamine, marked F, from those for complexed triamine, marked C (see Figure 14). The resonances for free triamine TMTAN show it to consist of at least three slowly interconverting conformers, at 160 K. From the shifts and intensities of the resonances assigned to complexed TMTAN, it appears that all three come from a single monomeric tridentately complexed Np$^6$Li with two N$^{13}CH_2$'s at $\delta$ 50.6 and 56.4 and one kind of N$^{13}CH_3$ at $\delta$ 46.5 in the ratio 1:1:1, respectively. A model of such a complex has been constructed (Figure 15) using bonding parameters obtained from published X-ray crystallographic structures of monomeric RLi–PMDTA complexes.[11] These parameters are the N–Li–N angle of 90° and N–Li bond distance of ca. 2.1 Å. In this model the ligand assumes a crown configuration with two types of alternating $NCH_2$ carbons distinguished by their distances from lithium. The three furthest from lithium each bear a C–H bond pointing down, away from lithium. All vicinal C–H bonds are staggered and three alternating methylene carbons carry bonds which eclipse bonds about the directly bonded nitrogen. The species has a $C_3$ axis and is chiral.[23] Actually the X-ray crystallographic structure of Co(III) coordinated to 1,4,7-triazacyclononane in the tripolyphosphate salt is very similar to the structure proposed in Figure 15 for the NpLi·TMTAN complex.[24]

Above 160 K with increasing temperature, the $^{13}C$ doublet due to N–$CH_2$ of NpLi complexed TMTAN averages to a line at its center. Line-shape analysis reveals that the process responsible for this signal averaging has a $\Delta H^{\ddagger}$ of 8 kcal/mol. The exchange rates are much faster than carbon–lithium bond exchange and exchange of TMTAN between the complex and its free state in solution. Both of these processes are slow even at 260 K, evidenced by well-resolved resonances for free and complexed TMTAN and still visible splitting of the neopentyl methylene $^{13}C$ resonance due to $^{13}C$, $^6Li$ coupling. Rather, the most likely origin of the averaging of $^{13}CH_2$ resonances in complexed TMTAN is internal motions in the complex induced by fast reversible local N, Li bond dissociation. This then causes the entire complexed triamine to invert between its two enantiomers.

## Conclusions

In general, dissociation of solvated organolithium compounds to smaller aggregates is accompanied by increased coordination to lithium and is favored at lower temperatures.[1,2,7-9] Evidently the exothermicity of extra coordination to lithium must overcome energies associated with the bridged C–Li–C bonds which cleave; see for example, eq 1. The progression of increased solvation and further dissociation runs from cubic tetramers, to bridged dimers, to tridentately bound monomers favored by, respectively, ordinary monoethers, vicinal diamines, and triamines with appropriately sited nitrogens (such as PMDTA). The hindered character of NpLi allows dimers to be formed in diethyl ether and monomers and dimers in THF. The latter is a superior ligand to diethyl ether and is also less hindered. Hence THF favors more dissociated species, dimers and monomers, than is usually found. THF in bulk is also a superior lithium coordinator to TMEDA and 1,2-di(*N*-piperidino)ethane as observed in competition experiments. Of special interest are the Np$^6$Li monomers tridentately complexed to triamines. These are dynamically stable in that carbon–lithium bond exchange, exchange of triamine between the complex and its free state in solution, and even rotation about the carbon–lithium bond are all quite slow compared to the behavior of other organolithium compounds complexed to monoethers, monoamines, and 1,2-diamines. This has allowed identification of the structures of the solvates and measurement of the rates of some of the above-mentioned dynamic processes; included among these is the rate of rotation about the carbon–lithium bond in the PMDTA solvated Np$^6$Li monomer, hitherto inaccessible to observation.

## Experimental Section

**NMR Experiment.** Lithium-6, $^{13}C$, and proton NMR was carried out with several Bruker NMR spectrometers (AM-240, AM-500, MSL-300, and WH-300) using our previously published instrumental parameters.[25]

**Neopentyllithium-$^6$*Li*.** Inside a glove box under an argon atmosphere a Schlenk flask was loaded with a magnetic stir-bar, dineopentylmercury[26] (7.04 g, 20.05 mmol), 40 mL of dry pentane free of oxygen, and finally clean thinly sliced lithium-6 (0.5 g, 83 mg-atoms). The flask was closed and the mixture stirred (in the glove box) for 3 days at room temperature. Then more $^6$Li was added (0.5 g 83 mmol). After several hours of stirring the solution turned cloudy, then black. The reaction mixture was stirred for 2 more weeks at room temperature, then filtered through a glass frit, and the precipitate washed with pentane. Caution: Hg(Li) is very flammable! The resulting brown-yellow solution was cooled, concentrated in vacuum, and filtered, yielding 1 g of white semicrystalline neopentyllithium-$^6$Li in 63% yield. This solid, stable for months in the glove box, was weighed into sample tubes for NMR investigation.

**Preparation of NMR Samples. Example of Neopentyllithium in THF–TMEDA.** Attached to the end of the 10-mm o.d., 8-in. NMR tube was a 14/20 female joint to connect with a straight bore stopcock with

(23) We are indebted to Professor J. M. Lehn, Université de Strasbourg, for pointing this out.
(24) Haight, G. P.; Hambley, T. W.; Hendry, P.; Lawrance, G. A.; Sargeson, A. M. *J. Chem. Soc., Chem. Commun.* **1985**, 488.
(25) Fraenkel, G.; Winchester, W. R. *J. Am. Chem. Soc.* **1989**, *111*, 3794.
(26) (a) Whitmore, F. C.; Rohrmann, E. *J. Am. Chem. Soc.* **1939**, *61*, 1591. (b) Fraenkel, G.; Appleman, B. *J. Am. Chem. Soc.* **1974**, *96*, 5113.

14/20 joints on each side. To protect the system, the stopcock joint farthest from the NMR tube was closed with a serum cap. Neopentyllithium (0.01 g, 13 mmol) was weighed into the NMR tube in the dry box (Vaccuum Atmospheres) under an argon atmosphere. The NMR tube was closed with the stopcock assembly, removed from the drybox, and cooled to −78 °C with dry ice–propanol. Meanwhile TMEDA, distilled from $CaH_2$ (0.03 g), was weighed in the drybox and dissolved in THF-$d_8$ (distilled from Na-K) (0.440 g). This mixture was drawn into a glass syringe, protected by a three-way luer valve with a septum blocking the side opening of the valve (the latter was closed to the syringe side), and dry argon was blown through the needle to remove traces of air. Then the needle was drawn through the protecting serum cap through the stopcock and as far as possible into the cooled NMR tube. The THF–TMEDA mixture was slowly syringed down the side of the NMR tube, cooling to −78 °C before it reached the neopentyllithium. After addition was complete, the NMR tube assembly (stopcock closed) was transferred to the vacuum line, its contents frozen with liquid nitrogen, and the tube evauated and sealed. The NMR study was begun within 24 h of sample preparation. The sample was precooled to 200 K, and NMR spectra were obtained at the lower temperatures first.

Other samples prepared as described above were neopentyllithium with (a) 1,2-di(*N*-piperidino)ethane in THF-$d_8$, stable at 200 K for 1 month; (b) PMDTA in THF-$d_8$; (c) PMDTA in diethyl-$d_{10}$ ether; (d) 1,4,7-trimetyl-1,4,7-triazacyclononane in THF-$d_8$. Unless otherwise stated all ligands were dried with Na/K immedately before distillation and preparation of samples.

**Samples Prepared by Vacuum Transfer of Solvent.** The following samples were prepared by bulb-to-bulb distillation of the solvent mixtures onto neopentyllithium in the NMR tubes, the latter cooled to 200 K: neopentyllithium in (a) methylcyclohexane-$d_{14}$, stable 6 months at room temperature; (b) THF-$d_8$, stable 1 week at 170 K; (c) diethyl-$d_{10}$ ether, stable 1 month at 200 K; (d) diethyl-$d_{10}$ ether–toluene-$d_8$, stable 1 month at 200 K; (e) 1,4,7-trimethyl-1,4,7-triazacyclononane in diethyl-$d_{10}$ ether 2 months at 250 K. The rest of these preparations were the same as descried for neopentyllithium in THF-$d_8$–TMEDA.

Sample concentration were determined from the mode of preparation and integration of the low-temperature $^{13}C$ NMR spectra. Correction for the inevitable small degree of hydrolysis was accomplished by integration of the $^{13}C$ neopentane resonances observed in some spectra.

**Acknowledgment.** This research was generously supported by National Science Foundation Grant Nos. CHE 8304636 and 8817746 and in part by the Goodyear Tire and Rubber Co. The National Science Foundation also supported acquisition of two high-field NMR spectrometers used in this work. We thank Dr. Charles Cottrell, Campus Chemical Instrumentation Center, for helpful technical advice.

# $^1H$ NMR Study of the Role of Individual Heme Propionates in Modulating Structural and Dynamic Properties of the Heme Pocket in Myoglobin

**Jón B. Hauksson, Gerd N. La Mar,* Ravindra K. Pandey, Irene N. Rezzano, and Kevin M. Smith**

*Contribution from the Department of Chemistry, University of California, Davis, California 95616.* *Received January 8, 1990*

**Abstract:** The relative importance of the two heme propionate salt bridges to the protein matrix in determining the equilibrium orientational preference of the synthetic hemin, heptamethyl–monopropionate–porphine–iron(III), reconstituted into sperm whale and horse myoglobin metcyano complexes was determined using the nuclear Overhauser effect, NOE. The preferences for occupying the crystallographic 7-propionate position which makes a link to interior His FG3 in both proteins, versus that of the 6-propionate group interacting with the surface CD3 residue, were found to be ~1:2 for the sperm whale and 3:2 for the horse protein. Since the FG3 residue is conserved (His), and the CD3 residue differs in the two proteins (Arg for sperm whale, Lys for horse), we conclude that the 6-propionate–Lys CD3 link in horse Mb is less stable by ~0.64 kcal/mol than the 6-propionate–Arg CD3 salt bridge in sperm whale Mb. Since this salt bridge, in part, holds closed a likely distal ligation channel to the heme pocket, the lower stability of this link in the horse relative to the sperm whale protein provides a structural basis for interpreting earlier highly differential labile hydrogen dynamics for the two proteins (Lecomte, J. T. J.; La Mar, G. N. *Biochemistry* **1985**, *24*, 7388–7395). Reconstitution of horse Mb with protohemin IX derivatives having individual propionates selectivity replaced by methyls confirms that vinyl contacts are much more important than propionate contacts in determining the orientational preference of the heme in the pocket. Each of the monopropionate hemins revealed that the orientational isomer with a propionate in the crystallographic 6-position is in dynamic equilibrium ($\sim 10^3$ $s^{-1}$) with another isomeric form which is deduced to be the heme orientation with the propionate in the crystallographic 8-position. The interconversion involves simply 90° rotational "hopping" of the heme about the iron–His bond, and this process is concluded to be significantly faster in the horse than sperm whale protein, again suggesting that the 6-propionate salt bridge is weaker in the former Mb.

## Introduction

The binding of the heme prosthetic group within the pocket of myoglobin, Mb, is determined by a number of heme–protein interactions. These include the axial imidazole–iron bond, van der Waals interactions between hydrophobic amino acid side chains and the polarizable heme $\pi$ system, salt bridges, and/or hydrogen bonds to the ubiquitous heme propionates, and possibly small steric influences resulting from protein constraints forcing vinyl side chains to be more in-plane than in model compounds.[1,2] It is possible to perturb significantly these heme–protein contacts and still retain strong heme binding as witnessed by the formation of strong holoprotein complexes in either the absence of a central metal to form the iron–His bond,[3] the esterification of both propionates,[4] or the wide range of chemical functionalization of

(1) Antonini, E.; Brunori, M. *Hemoglobin and Myoglobin in Their Reactions with Ligands*; North Holland Publishing Co.: Amsterdam, 1971; Chapter 13.

(2) (a) Takano, T. *J. Mol. Biol.* **1977**, *110*, 537–568. (b) Takano, T. *J. Mol. Biol.* **1977**, *110*, 569–584. (c) Phillips, S. E. V. *J. Mol. Biol.* **1980**, *142*, 531–534. (d) Kuriyan, J.; Wilz, S.; Karplus, M.; Petsko, G. A. *J. Mol. Biol.* **1986**, *192*, 133–154.

(3) Jameson, D. M.; Gratton, E.; Weber, G.; Alpert, B. *Biophys. J.* **1984**, *65*, 795–803.

(4) Tamura, M.; Asakura, T.; Yonetani, T. *Biochim. Biophys. Acta* **1973**, *295*, 467–479.

0002-7863/90/1512-6198$02.50/0 